THE PENNSYLVANIA STATE UNIVERSITY
SCHREYER HONORS COLLEGE

DEPARTMENT OF CHEMICAL ENGINEERING

AN EXPLORATION OF THE ULTRAFILTRATION BEHAVIOR OF HIGHLY CONCENTRATED MONOCLONAL ANTIBODY SOLUTIONS

STEPHANIE NITOPI
SPRING 2014

A thesis
submitted in partial fulfillment
of the requirements
for a baccalaureate degree
in Chemical Engineering
with honors in Chemical Engineering

Reviewed and approved* by the following:

Andrew Zydney
Walter L. Robb Chair and Professor of Chemical Engineering
Thesis Supervisor

Michael Janik
Associate Professor of Chemical Engineering
Honors Adviser

* Signatures are on file in the Schreyer Honors College.

ABSTRACT

Monoclonal antibodies (mAbs) are a major class of bio–therapeutic proteins with wide ranging applications in treating autoimmune diseases and cancer. Highly concentrated doses are typically needed to achieve the desired therapeutic effect given the volume limitations of subcutaneous injections. Ultrafiltration is currently used for purification and concentration of protein solutions in the pharmaceutical industry. However, there are significant challenges in applying ultrafiltration to achieve very high protein concentrations due to membrane fouling and concentration polarization effects. The objectives of this work were to explore the behavior of ultrafiltration processes at very high concentrations of a highly purified monoclonal antibody (provided by Amgen) and to determine the mechanisms controlling the filtrate flux. Ultrafiltration data were obtained in both tangential flow filtration (TFF) and stirred cell (SC) experiments. In addition, the osmotic pressure was evaluated as a function of protein concentration and buffer conditions to provide a direct measure of the effects of protein–protein interactions on the thermodynamic properties of highly concentrated antibody solutions. The filtration data clearly show that there is a maximum attainable protein concentration corresponding to the point where the filtrate flux goes to zero. The measured flux is in good qualitative agreement with predictions of the concentration polarization model, although the behavior at very high protein concentrations is more complicated due to the large variation in transmembrane pressure associated with the high viscosity of the antibody solution. These studies provide important insights into the factors that govern the performance of ultrafiltration processes for highly concentrated antibody solutions.

TABLE OF CONTENTS

LIST OF FIGURES

LIST OF TABLES

ACKNOWLEDGEMENTS

The author would like to acknowledge Amgen, Inc. for donation of the monoclonal antibody and for their financial support, as well as thank EMD Millipore for donation of the Ultracel membranes and Pellicon 3 modules. The author would like to thank Elaheh Binabaji for her mentoring and assistance with experiments, and Dr. Andrew Zydney for his guidance, insights, and support.

Chapter 1

Introduction

Membranes have played a major role in bioprocessing since the start of the biotechnology industry. Early biopharmaceutical products were highly active hormones (e.g., insulin), thrombolytic agents, and clotting factors, which were required at relatively low dose and typically had low annual production levels of less than 1 kg per year [1]. The early membranes and systems used by the biotechnology industry were adopted from technologies developed by the food, dairy, and water industries [1]. Over the past few decades, the biotechnology industry has evolved greatly, and as a result, there have been rapid developments in membrane technologies specifically targeted to the demands in bioprocessing.

One particular trend that has gained momentum over the past ~20 years is the development and successful commercialization of therapeutic monoclonal antibodies (mAbs). As of 2005, there were a total of 18 FDA approved mAbs, and they comprised the majority of recombinant proteins in clinical studies (more than 150 products worldwide) [2]. According to the Antibody Society, there are now more than 35 FDA approved therapeutic mAbs as of January 2014 [3]. Most mAbs are targeted to one of three major therapeutic categories: oncological, immunological, and anti–infective [2]. These molecules bind stoichiometrically to a particular receptor or cell type, and thus require much higher dosing levels than early recombinant protein products that act catalytically or as signaling agents. Current annual production levels for most mAbs are as high as 1000 kg [4]. Another challenge in the purification of monoclonal antibodies is the large range of impurities that need to be removed

including host cell proteins, DNA, and aggregated forms of the desired product. Purity requirements vary for different products, but typical targets for monoclonal antibody products are in the ppm range (e.g., micrograms of host cell proteins per gram of antibody product), requiring very efficient and effective separations [4]. The shifting landscape of bioproducts, as well as the increased dosing, production, and purity requirements of monoclonal antibody products, has created significant challenges for downstream bioprocessing.

Membrane processes are used extensively for a variety of bioprocessing steps, including sterile filtration, initial harvest, virus removal, protein concentration, buffer exchange, and protein purification [4]. One membrane process of particular importance is ultrafiltration, which has become the method of choice for concentration and formulation of final bulk protein products in the biotechnology industry [5]. Ultrafiltration membranes typically have pore sizes between 1 – 20 nm and are designed to retain macromolecules, such as proteins, and pass small solutes and water [4]. The membranes utilized for ultrafiltration are typically characterized based on their nominal molecular weight cut–off (MWCO), which is defined as the molecular weight of a protein that is 90% retained by the membrane. While ultrafiltration has typically been viewed as a purely size–based separation process, recent work has shown that charged membranes can be used to increase selectivity by exploiting electrostatic interactions between the protein and membrane [6].

There are two main types of filtration configurations: normal flow filtration (NFF) and tangential flow filtration (TFF). NFF is primarily used for systems at very low concentrations. TFF, in which the feed flow is directed parallel to the membrane and perpendicular to the filtrate flow, can be used for higher concentrations of retained species and can also achieve a higher filtrate flux compared to NFF [7]. One challenge with tangential flow filtration, however, is that

the transmembrane pressure drop varies with position along the length of the module due to frictional losses, an effect that is particularly pronounced at high protein concentrations due to the high viscosity of the resulting solutions.

The filtrate flux during ultrafiltration (volumetric filtrate flow rate divided by the membrane area) may be decreased due to membrane fouling and / or concentration polarization effects. Membrane fouling refers to clogging of the membrane pores or deposition of solute onto the surface of the membrane, e.g., through the formation of a "cake layer". Concentration polarization refers to the accumulation of solute within a boundary layer above the membrane surface, forming a concentration gradient. This results in a reduction in the effective pressure driving force for filtration due to osmotic pressure effects [4].

The filtrate flux is typically described in two limiting regimes: the pressure–dependent and the pressure–independent regimes. At very low transmembrane pressures, concentration polarization effects are minimal, and the filtrate flux is governed by the membrane permeability (L_p) and the effective pressure driving force [7]:

$$J_v = \left(\frac{L_p}{\mu}\right)(\Delta P - \sigma\Delta\Pi) \qquad (1)$$

where J_v is the filtrate flux, L_p is the membrane permeability, μ is solvent viscosity, ΔP is the transmembrane pressure, σ is the osmotic reflection coefficient, and $\Delta\Pi$ is the osmotic pressure difference associated with the bulk protein concentration assuming that the wall concentration (C_w) is approximately equal to the bulk concentration (C_b) at low pressures. The permeability is typically a function of the membrane pore size distribution, porosity, and thickness. The membrane permeability can be obtained from the slope of a plot of the filtrate flux versus the transmembrane pressure; this is typically done with buffer in which the osmotic reflection coefficient is zero for all solutes.

The filtrate flux in the pressure–independent regime is assumed to be limited by mass transfer effects. The flux under these conditions is typically evaluated using the stagnant film model [7]:

$$J_v = k_m \ln\left(\frac{C_w}{C_b}\right) \quad (2)$$

where k_m is the protein mass transfer coefficient, and C_w and C_b are the protein concentrations at the membrane surface and in the bulk solution, respectively. A plot of the filtrate flux versus the logarithm of the bulk concentration can be used to obtain the mass transfer coefficient, which corresponds to the absolute value of the slope of the linear regression fit. The wall concentration is usually assumed to be constant at a value equal to the protein solubility limit or to the concentration needed for the protein osmotic pressure to be approximately equal to the applied transmembrane pressure. Thus, the maximum wall concentration can be estimated from the linear regression fit based on the x–intercept.

The mass transfer coefficient is a function of the device geometry, hydrodynamics, feed flow rate, and protein diffusion coefficient (which is in turn dependent on protein charge, buffer conductivity, and protein concentration) [4]. In addition, the protein diffusion coefficient and mass transfer coefficient can be functions of the protein concentration, particularly at high protein concentrations, due to the effects of protein–protein interactions on diffusion and the solution viscosity.

Osmotic pressure measurements can provide important information on the behavior of highly concentrated monoclonal antibody solutions because the osmotic pressure has a direct effect on the flux during protein ultrafiltration due to the reduction in the effective pressure driving force (Equation 1), particularly at high degrees of concentration polarization [8, 9]. In

addition, osmotic pressure data can provide a measurement of higher order multi–body interactions [10], which can be particularly important at the very high protein concentrations that exist near the membrane surface.

The push for lower production costs, increased development speed, and overall higher productivity in the biotechnology industry requires further improvements in downstream bioprocessing. One particular challenge lies in achieving the very high protein concentrations required for the formulation of therapeutic monoclonal antibodies. The objectives of this work were to explore the behavior of ultrafiltration processes at very high protein concentrations using a highly purified monoclonal antibody with the goal of determining the mechanisms controlling the filtrate flux and the factors governing the maximum achievable protein concentration. This knowledge could lead to improved methods for formulating highly concentrated monoclonal antibody solutions, which would have far–reaching implications in the biopharmaceutical industry.

Chapter 2

Materials and Methods

2.1 Protein Solution Preparation

A highly purified monoclonal antibody was provided by Amgen, Inc. with a molecular weight of 142 kDa and an isoelectric point of 8.1. The antibody solution was stored at –80°C and slowly thawed prior to use. The antibody was placed in the desired buffer solution for each experiment using a buffer exchange process. This was accomplished by constant volume diafiltration through fully retentive Ultracel^{TM} composite regenerated cellulose membranes with a nominal molecular weight cut–off of 10 kDa (Millipore Corp., Bedford, MA). The resulting protein solution was kept at 4°C and typically used within seven days of preparation. Solutions were stored for longer durations at –30°C as needed.

2.2 Buffer Solution Preparation

Buffered salt solutions were prepared by dissolving appropriate amounts of sodium acetate (Sigma, S7670), sodium phosphate monobasic (Sigma, S9638), and/or sodium phosphate diabasic (Sigma, S7907) in deionized water obtained from a NANOpure® Diamond water purification system (Barnstead Thermolyne Corporation Dubuque, IA). Some data were also obtained with sucrose (Sigma, S-2395) and L-proline (Spectrum Chemical, P1434) added as excipients. The ionic strength of all buffer solutions was adjusted using NaCl (BDH Chemicals, BDH0286) and was measured with a 105 A Plus conductivity meter (Thermo Orion, Beverly,

MA). The pH was adjusted to the desired value using HCl or NaOH as needed. All buffer solutions were prefiltered through 0.2 µm Supor® 200 membranes (Pall Corp., Ann Arbor, MI) to remove any undissolved salt or particulates prior to use.

2.3 Protein Concentration Measurements

Two methods were used to measure the protein concentration. For the majority of experiments, concentrations were determined spectrophotometrically using a SPECTRAmax Plus 384 UV-Vis spectrophotometer at an absorbance of 280 nm. Protein samples obtained during experiments were diluted as needed to ensure that the measured absorbance was in the linear range (absorbance between 0.1 and 0.4). Actual concentrations were then evaluated by comparison of the absorbance with that of known protein standards. At least three repeat measurements were taken, and the results were reported as the mean ± standard deviation of these measurements.

Alternatively, protein concentrations were determined with a NanoDrop 2000 UV-Vis microvolume spectrophotometer using pre–configured software for Protein A280 assays (Type: other protein [E: 1%], Ext. Coeff [E 1% L/gm-cm] = 15.85). 4 µL samples were loaded into the NanoDrop 2000 for all concentration measurements. The two methods gave very similar results; the NanoDrop 2000 was used for the stirred cell experiments due to the very small filtrate volumes available for analysis.

2.3 Membrane Permeability Measurements

The permeability of the membrane was measured before and after every experiment to check the extent of fouling. This was accomplished by measuring the filtrate flux as a function of transmembrane pressure (TMP). The filtrate flux was evaluated volumetrically by measuring the amount of permeate that passed through the membrane during a given time period. Data were analyzed using the classical membrane transport model, Equation 1. The permeability was measured using deionized water, so the osmotic pressure term should equal zero. Therefore, a plot of filtrate flux vs transmembrane pressure yields a straight line with slope equal to L_p/μ.

2.5 Osmotic Pressure Experiments

2.5.1 Membrane Preparation

The protein osmotic pressure was evaluated using a membrane osmometer containing an Ultracel^{TM} composite regenerated cellulose membrane with a nominal molecular weight cut–off of 30 kDa (Millipore Corp., Bedford, MA). The membrane disc was prepared by first soaking in 90% isopropanol for 45 minutes to fully wet the pores. The membrane disc was then rinsed with DI water and flushed with at least 100 mL of DI water at a pressure of 30 kPa (4.5 psi).

2.5.2 Assembling the Membrane Osmometer

A schematic of the membrane osmometer is shown in Figure 1. The device consisted of two Plexiglas chambers, each with a volume of approximately 12 mL. The two chambers were

separated by the previously prepared 30 kDa membrane, which has an effective surface area of 3.1 cm^2. The membrane was placed in a membrane holder on top of a porous Tyvek support and sealed with two O-rings. The membrane holder was placed in the feed chamber, and the two chambers were screwed together. The upstream (feed) chamber was filled with the protein solution, and the downstream (buffer) chamber was filled with the same buffer used to prepare the protein solution. Any entrapped air was removed by gently rotating and tapping the device. The upstream chamber was then connected to a feed reservoir, which in turn was connected to a pressurized air valve to control the transmembrane pressure in the system (determined by a digital pressure gauge). The membrane osmometer was placed in a holder and raised to the height of the feed chamber. An outlet capillary tube (inner diameter = 1.6 mm) was attached to the buffer chamber to measure filtrate flux by volumetric displacement. All experiments were performed at room temperature.

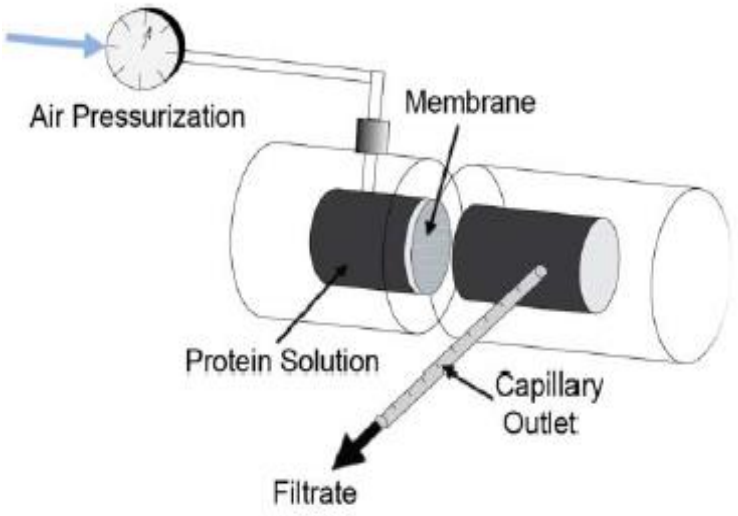

Figure 1: Membrane Osmometer Schematic
Reproduced from [10]

2.5.3 Osmotic Pressure Measurements

The osmotic pressure of the protein solution at various antibody concentrations was evaluated as follows. The steady state filtrate flux (J_v) was measured as a function of transmembrane pressure (ΔP). Applied pressures below the osmotic pressure resulted in a backwards (negative) flow of filtrate, with the meniscus in the outlet capillary tube moving back towards the outlet port. Applied pressures above the osmotic pressure resulted in a forward (positive) flow. The osmotic pressure was determined from a plot of the filtrate flux as a function of transmembrane pressure, with the x-intercept (corresponding to $J_v = 0$) evaluated by simple linear regression. The osmotic pressure was then calculated from Equation (1) assuming that the osmotic reflection coefficient of the 30 kDa membrane was equal to one.

2.6 Tangential Flow Filtration Experiments

Tangential Flow Filtration (TFF) experiments were performed using a Pellicon 3 cassette containing 88 cm^2 of an Ultracel™ composite regenerated cellulose membrane with a nominal molecular weight cut–off of 30 kDa. A schematic of the experimental apparatus is shown in Figure 2. The cassette was installed in the cassette holder as described in the user manual provided by Millipore. The module was initially flushed with deionized water using at least 60 L/m^2 to ensure removal of the shipping / storage solution. The membrane was then cleaned by washing with 0.3 M NaOH at pH 10.5 for 60 min at a feed flow rate of 45 mL/min.

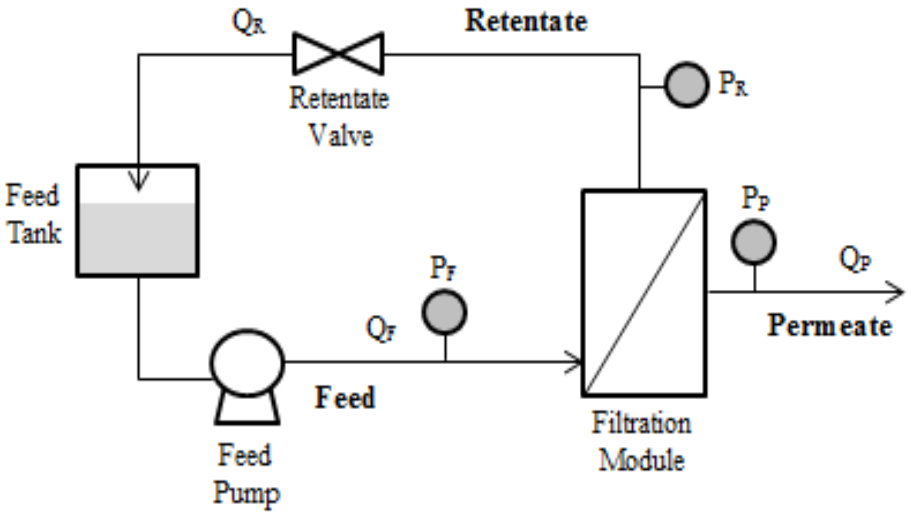

Figure 2: Tangential Flow Filtration Schematic

Before each experiment, the module was washed with 0.1 M NaOH for approximately 10 min under total recirculation (permeate and retentate both recycled back to feed tank). Approximately 200 mL of DI water was then flushed through the system (no recirculation) to remove residual NaOH, followed by washing with DI water (with recirculation). Lastly, the module was washed with the buffer solution to be used in the ultrafiltration experiment. At the end of each experiment, the module was emptied, and a small amount of buffer solution (~20 mL) was recycled through the module to collect any remaining protein solution; this was recombined with the bulk solution to minimize protein losses. The module was then flushed with buffer, DI water without recirculation, and DI water with recirculation. The module was stored between experiments either filled with DI water or with 0.1 M NaOH; the NaOH was used whenever the membrane permeability was more than 30% below that of the value determined for the clean membrane.

2.6.1 Total Recycle Experiments

Total recycle experiments were performed using the module in a closed loop configuration, with both the retentate and permeate returned to the feed tank to maintain constant antibody concentration. The filtrate flux was evaluated as a function of the transmembrane pressure over a range from about 20 – 140 kPa (3 – 20 psi). Data were typically obtained at a single feed flow rate over a range of protein concentrations (feed diluted with buffer after each pressure excursion). In some experiments, data were obtained at multiple feed flow rates before changing the protein concentration.

2.6.2 Standard Batch Filtration Experiments

Batch filtration experiments were performed at a constant transmembrane pressure of 107 kPa (15.5 psi) and a constant feed flow rate of 25, 35, 45, 55, or 65 mL/min. The module was operated in an open loop configuration, with the retentate recycled back to the feed tank while the permeate was removed. In each case, the filtrate flux was evaluated as a function time corresponding to continually increasing values of the protein concentration. The retentate pressure (P_R) was adjusted as the feed solution became more concentrated (and thus more viscous) to keep the mean transmembrane pressure essentially constant throughout the experiment. The filtrate flux and antibody concentration were evaluated every 3–5 min, as described previously.

2.6.3 Modified Batch Filtration Experiments

To reduce the number of experiments and conserve protein, the standard batch experiments were modified as follows. Instead of keeping the feed flow rate constant throughout the experiment, 1 to 3 data points were obtained at a given feed flow rate at which point the feed flow rate was rapidly increased (or decreased). The system was allowed to stabilize for several min, with the filtrate flux and antibody concentration then evaluated at this new feed flow rate at several time (concentration) points. This procedure was repeated multiple times, with the feed flow rate alternated between 35, 45, and 55 mL/min.

2.7 Stirred Cell Ultrafiltration Experiments

Stirred cell (SC) experiments were performed in a 200 mL Amicon stirred cell, Model 8200 (Cat. No. 5123). An Ultracel^{TM} composite regenerated cellulose membrane with a nominal molecular weight cut–off of 30 kDa and an effective surface area of 28.7 cm^2 was placed in the bottom of the cell. The filtrate flux was measured as a function of protein concentration as the solution became more concentrated over time. Data were obtained at a single transmembrane pressure (59 kPa = 8.5 psi) and either a stirring speed of 600 or 300 rpm. The pressure was determined by a digital pressure gauge. The stirring speed was evaluated by a Type 1531 Strobotac® Electronic Stroboscope. The stroboscope was also used to evaluate the stirring speed at several points during the protein ultrafiltration experiment to determine if the increase in solution viscosity at high antibody concentrations caused any changes in the stirring speed.

Chapter 3

Osmotic Pressure Experiments

As discussed in Chapter 2, the filtrate flux in the membrane osmometer was measured at several values of the transmembrane pressure to determine the osmotic pressure for a given monoclonal antibody solution. Typical data for a protein solution with an antibody concentration of 69 g/L are shown in Figure 3. The data are highly linear as expected, with the osmotic pressure evaluated from the x-intercept using simple linear regression as 1.4 kPa.

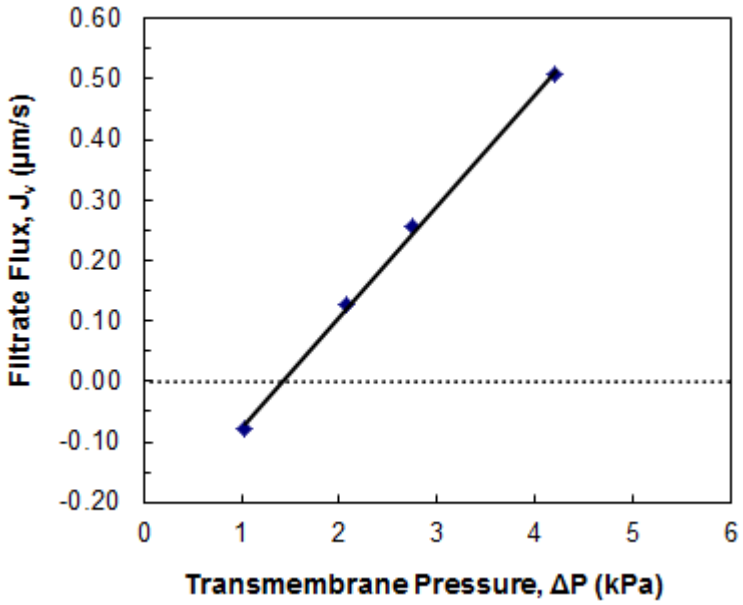

Figure 3: Osmotic pressure data at a concentration of 69 g/L
(5 mM sodium acetate, 100 mM NaCl, pH 5)

For solutions at higher protein concentrations (>100 g/L), the filtrate flux was very unstable leading to high variability in the data, especially at pressures well above or below the osmotic pressure. The flux was measured several times at each pressure until the system attained a steady state, which often required as much as 120 min. This long equilibration time is likely

associated with the development of the concentration polarization boundary layer in the solution immediately adjacent to the membrane. Figure 4 shows experimental results for a 300 g/L solution. Although there is considerable scatter in the data, the osmotic pressure could still be evaluated from the x–intercept, giving a value of approximately 14 kPa at this concentration.

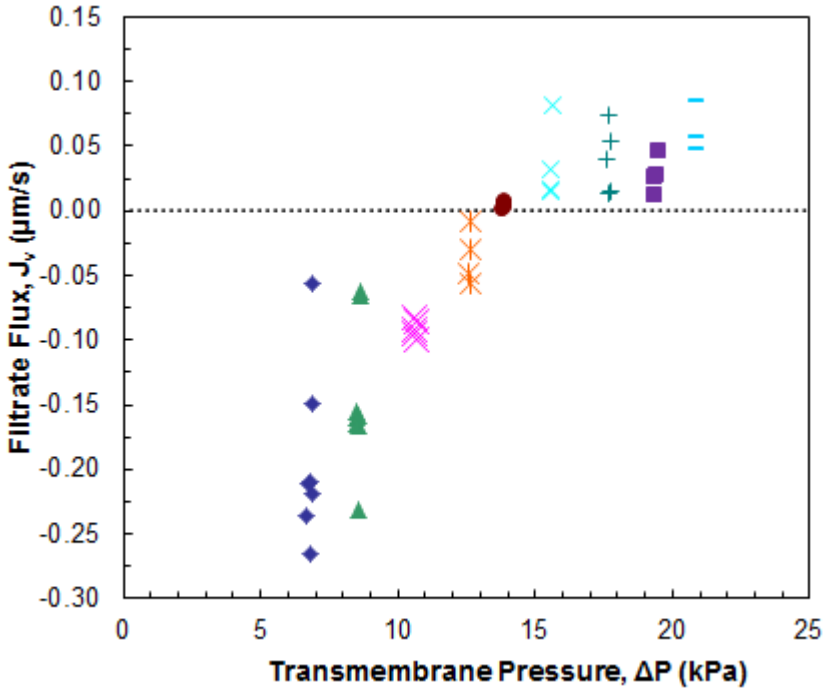

Figure 4: Osmotic pressure data at a concentration of 300 g/L
(5 mM Sodium Acetate, 100 mM NaCl, pH 5)

The osmotic pressure data obtained in this thesis were combined with more extensive measurements obtained by Elaheh Binabaji, with the results reported in [10]. Data for the osmotic pressure at pH 5 and three different ionic strength are shown in Figure 5 (taken from [10]). Note that the data at very high concentrations were obtained using a different experimental method (stirred cell) due to the difficulties encountered in this thesis in evaluating the osmotic pressure from the membrane osmometer data in Figure 4. The osmotic pressure increases significantly with increasing antibody concentration, with higher values obtained at the lower

ionic strength due to the increase in repulsive interactions between the positively charged antibody molecules at this pH.

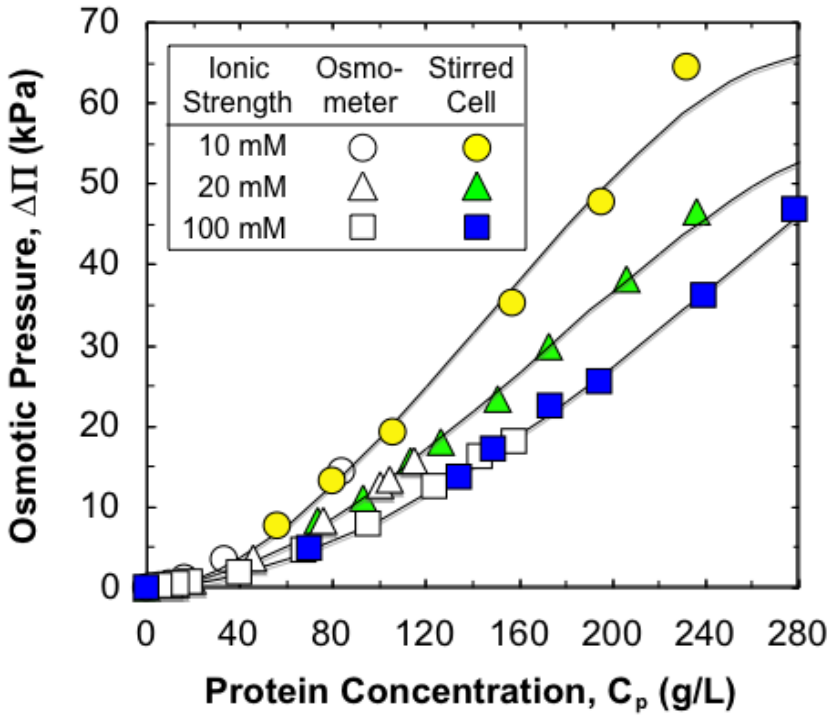

Figure 5: Osmotic pressure as a function of mAb concentration in acetate buffer at pH 5 with different NaCl concentrations. Reproduced from [9].

The osmotic pressure data were analyzed using a virial expansion of the form [10, 11]:

$$\Pi = RT\left\{2\left[\left(\frac{ZC_p}{2M_p}\right)^2 + m_s^2\right]^{\frac{1}{2}} - 2m_s\right\} + RT\left(B_1C_p + B_2C_p^2 + B_3C_p^3 + etc\right) \qquad (3)$$

where C_p and M_p are the protein concentration and molecular weight, m_s is the molar salt concentration, and the B_i are osmotic virial coefficients. The first term in Equation (3) is the Donnan contribution arising from the unequal partitioning of the electrolyte between the two sides of the membrane. The osmotic pressure data show signficant downward curvature at high

protein concentrations, corresponding to negative values of the third virial coefficient (B_3). This behavior is discussed in more detail by Binabaji et al. [10].

In summary, the membrane osmometer provided an accurate method for measuring the osmotic pressure for antibody concentrations up to around 100 g/L, but was difficult to apply for more concentrated solutions due to the instability in the filtrate flux and the corresponding difficulty in evaluating the x-intercept. The very low values of the filtrate flux were also difficult to evaluate accurately due to the small displacement of the meniscus, the long equilibration times, and possible artifacts associated with water evaporation within the capillary tube used to measure the volumetric displacement. A more detailed discussion of the experimental methods and the osmotic pressure data is available in [10].

Chapter 4

Tangential Flow Filtration Experiments

Tangential flow filtration (TFF) experiments were performed to study the effect of the protein concentration and feed flow rate on the ultrafiltration behavior of highly concentrated monoclonal antibody solutions. Data were obtained using: (1) total recycle experiments, in which the system was operated at steady state with both the permeate and retentate recycled back to the feed tank, (2) standard batch ultrafiltration experiments, in which the antibody concentration increased over time as permeate was removed by operating the system in an open loop mode with the retentate recycled, and (3) a modified batch ultrafiltration system that allowed data to be obtained at multiple feed rates in a single experimental run.

4.1 Total Recycle Experiments

Total recycle experiments were used to evaluate the ultrafiltration behavior at steady state. Figure 6 shows typical data from a total recycle experimental performed with a 20 g/L solution of the monoclonal antibody in a 5 mM sodium acetate, 20 mM NaCl buffer at pH 5 at two different feed flow rates: 45 and 55 mL/min. In both cases, the filtrate flux initially increases with increasing transmembrane pressure (in the pressure–dependent regime) and then appears to approach a pressure–independent value at high transmembrane pressures. The pressure–independent filtrate flux is greater at the higher feed flow rate (55 mL/min), consistent with an increase in the mass transfer coefficient (Equation 2). In addition, the pressure at which the flux transitions to the pressure–independent regime is shifted to a greater value.

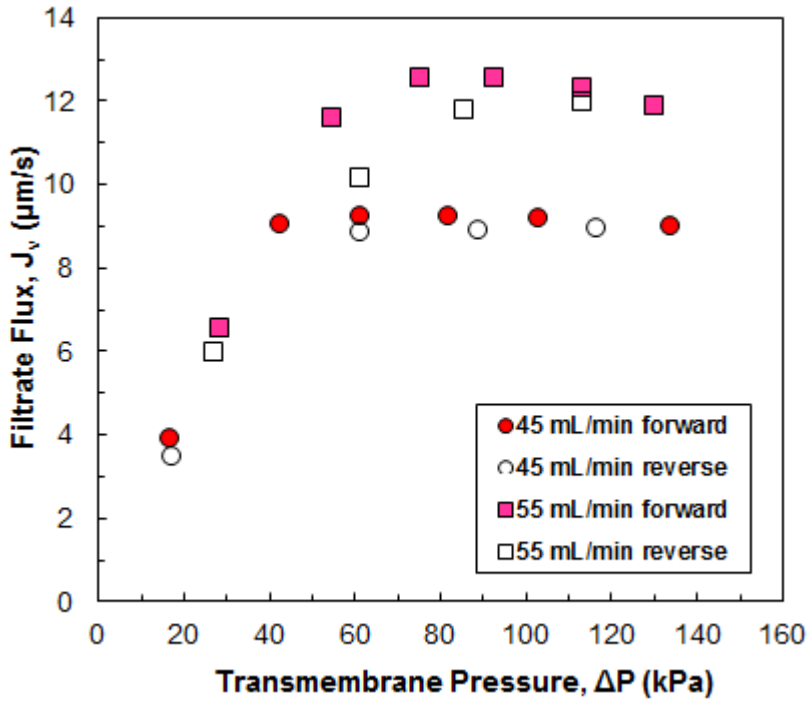

Figure 6: Total recycle results for a 20 g/L protein solution at two feed flow rates (5 mM sodium acetate, 20 mM NaCl, pH 5)

After reaching the highest transmembrane pressure (around 130 kPa = 19 psi), the transmembrane pressure was gradually reduced with the filtrate flux evaluated at each pressure after the system was allowed to stabilize (typically 2 min at a given pressure). The filtrate flux in this return cycle was nearly identical to that obtained with increasing pressure for the experiment performed with a feed flow rate of 45 mL/min. However, the system exhibited some hysteresis for the run at 55 mL/min with the flux during the return cycle falling somewhat below that obtained with increasing pressure. This reduction in flux may be due to some type of membrane fouling, which would reduce the membrane permeability.

Since our primary interest was in the effects of bulk protein concentration and feed flow rate on the filtrate flux, subsequent experiments were performed using a batch filtration (open loop) system in which the retentate is recycled back to the feed reservoir while the permeate is

removed (see next section). The system is operated at a constant transmembrane pressure, with the filtrate flux assumed to be at quasi–steady state throughout the batch process. In order to verify the quasi–steady assumption, filtrate flux data were obtained with the same TFF module in both total recycle and batch filtration modes at a feed flow rate of 35 mL/min, with the results summarized in Table 1. The filtrate flux data from the two different experimental methods are in good agreement, confirming that the flux during the batch filtration attains its steady state value at each bulk concentration. However, it should be noted that the filtrate flux data in Table 1 are much lower than the results presented later in this thesis. The exact cause of this discrepancy is unknown. The results presented in this section were from early experiments in which the key methods were still being established. It is also possible that there were some issues in measuring the protein concentrations. In addition, there were some problems with protein aggregation and membrane fouling in these experiments, which could have influenced the filtrate flux data.

Table 1: Filtrate flux in the batch and total recycle systems at a pressure of 107 kPa (15.5 psi) and a feed flow rate of 35 mL/min

C_b (g/L)	Filtrate Flux (μm/s)	
	Total Recycle	**Batch**
20	5.0	4.8
30	3.5	3.5
46	2.5	2.3
67	1.7	1.5

4.2 Standard Batch Filtration Experiments

Standard batch filtration experiments were conducted using an open loop configuration, in which the retentate was recycled back to the feed tank while the permeate was removed.

Figure 7 shows typical data for the filtrate flux (closed symbols) and antibody concentration (open symbols) as a function of time during a batch experiment performed at a feed flow rate of 45 mL/min for the antibody in a buffer containing 5 mM sodium acetate and 20 mM NaCl at pH 5. The filtrate flux at the beginning of the experiment was slightly above 15 µm/s (54 L/m^2/hr), but this decayed to approximately 1 µm/s (3.6 L/m^2/hr) at the end of the 50 min filtration. This reduction in the filtrate flux was a direct result of the increase in bulk protein concentration from 20 g/L at the start of the experiment to 180 g/L after 50 min. The membrane permeability evaluated at the end of this experiment was only slightly smaller than the initial permeability (within 20%), indicating that membrane fouling was relatively unimportant during the ultrafiltration.

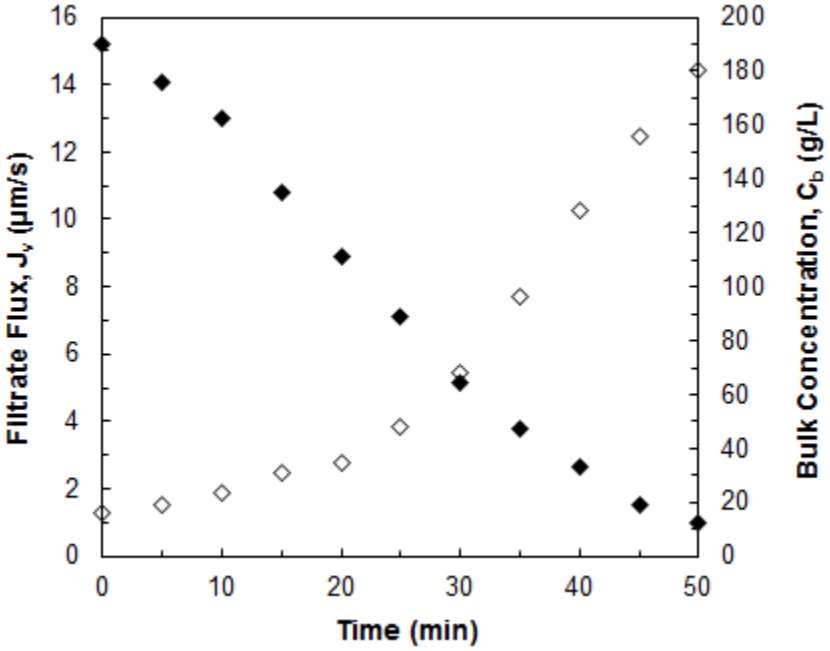

Figure 7: Raw data from a standard batch filtration experiment (45 mL/min) (5 mM sodium acetate, 20 mM NaCl, pH 5)

The experimental data in Figure 7 have been re–plotted in Figure 8 with the filtrate flux shown as an explicit function of protein concentration. The bulk concentration is plotted on a

logarithmic scale, consistent with the form given by the stagnant film model (Equation 2). This allows for the determination of the best fit values of the maximum wall concentration and mass transfer coefficient using a simple linear regression fit on the semi–log plot; this is discussed in more detail in the next section.

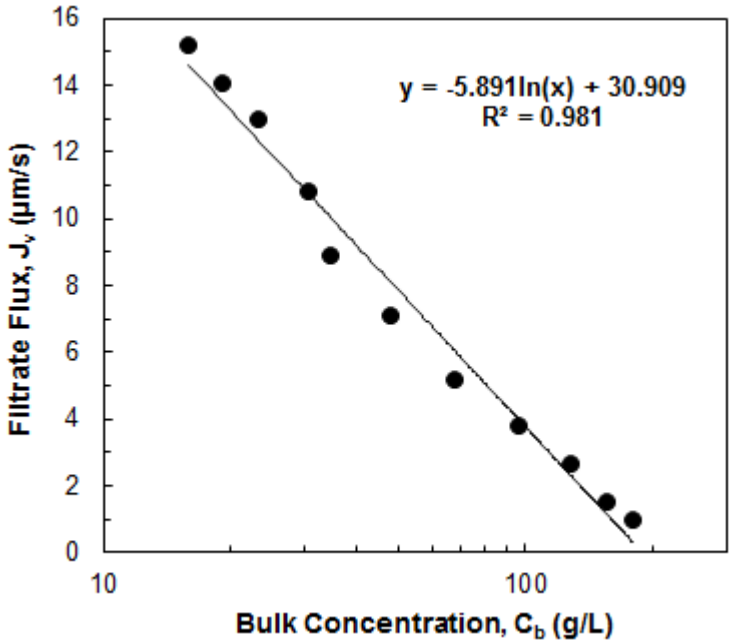

Figure 8: Filtrate flux vs bulk concentration (45 mL/min)
(5 mM sodium acetate, 20 mM NaCl, pH 5)

Figure 9 shows results from 5 separate batch filtration experiments each conducted at a different feed flow rate. The flux decreases with increasing protein concentration, with a nearly linear dependence on Log(C_b) as given by Equation (2). All of the data extrapolate to a point of zero filtrate flux at a bulk concentration somewhat less than 200 g/L. Note that for this buffer condition (5 mM sodium acetate and 20 mM NaCl at pH 5) the osmotic pressure of a 200 g/L solution of the mAb is approximately 38 kPa [10], which is considerably less than the applied transmembrane pressure in the batch filtration experiments (107 kPa).

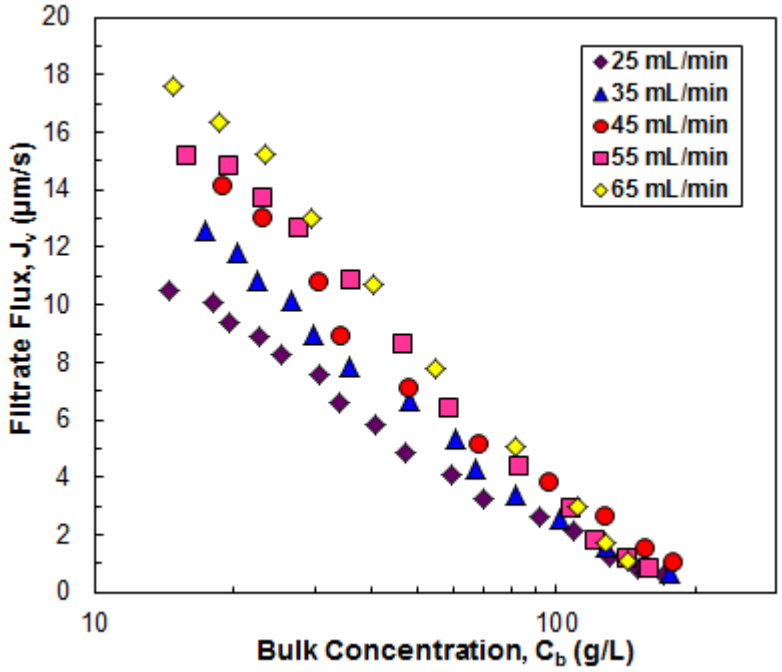

Figure 9: Filtrate flux as a function of bulk protein concentration during standard batch filtration

The best fit values of the maximum protein concentration determined from the data in Figure 9 are summarized in Table 2. There is no obvious dependence on the feed flow rate, with values of C_{max} ranging from 160 to 190 g/L.

Table 2: Best fit values of the maximum protein concentration in a 5 mM sodium acetate and 20 mM NaCl solution at pH 5.

Feed Flow Rate (mL/min)	Max C_w (g/L)
25	170
35	170
45	190
55	170
65	160

In order to see the effect of feed flow rate on the filtrate flux more clearly, the raw data from these experiments are replotted in Figure 10 as an explicit function of the feed flow rate for

several concentrations. The filtrate flux increases as the feed flow rate increases, consistent with the expected increase in the bulk mass transfer coefficient with increasing flow rate. The data at low mAb concentrations are highly linear, with slopes of approximately 0.15, which is much smaller than the value of around 0.5 that would be expected for flow in this type of screened channel [7]. The dependence on feed flow rate is even weaker at the higher protein concentrations, with considerable scatter in the data at 105 and 155 g/L. This behavior may be related to the very large transverse pressure drop that occurs through the module under these conditions. For example, at a protein concentration of 15 g/L, the pressure drop through the module at a feed flow rate of 25 mL/min is only 28 kPa, but this increases to more than 220 kPa at a protein concentration of 155 g/L due to the large increase in solution viscosity. This is discussed in more detail subsequently.

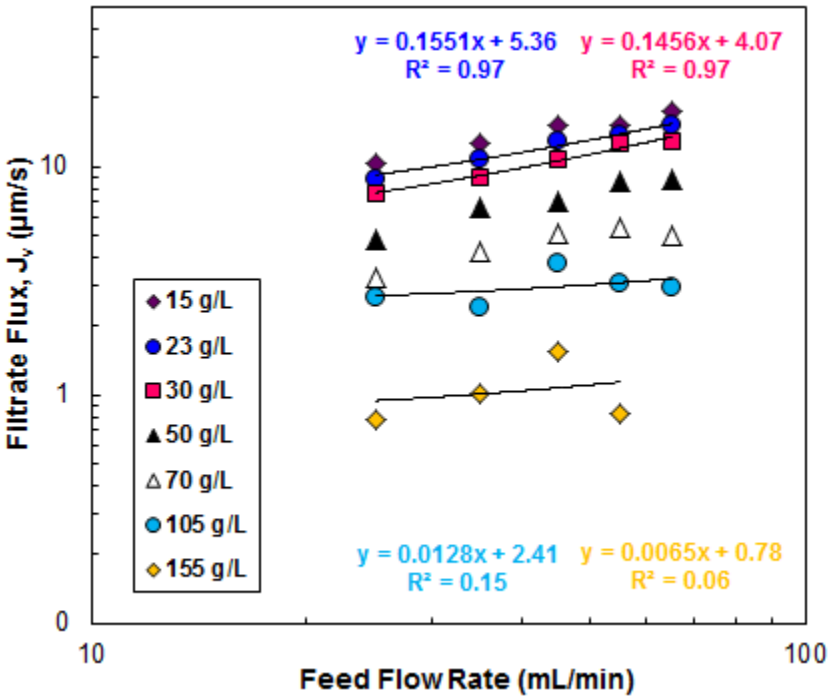

Figure 10: Filtrate flux as a function of feed flow rate at several values of bulk protein concentration

The effect of protein concentration on the pressure drop through the module is shown in Figure 11. All of the data were obtained at a mean transmembrane pressure of approximately 107 kPa (15.5 psi). Thus, for the runs at high protein concentrations, the exit transmembrane pressure drop was approximately zero (or even slightly negative), with the inlet transmembrane pressure drop approximately equal to the pressure drop through the module. The pressure drop increased significantly with increasing feed flow rate at low mAb concentrations as expected, although the dependence on feed flow rate was much less pronounced at higher mAb concentrations.

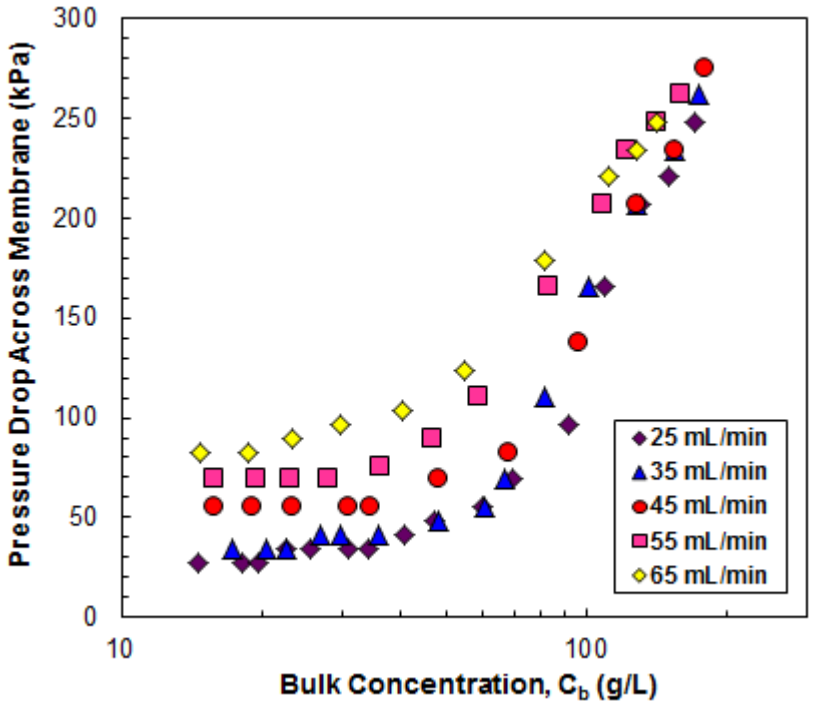

Figure 11: Pressure drop across the membrane during standard batch filtration experiments

The filtrate flux data at different feed flow rates are examined more carefully in Figure 12, which shows a plot of the ratio of the fluxes at different feed flow rates as a function of bulk protein concentration. At low protein concentrations, the flux ratios are less than one, consistent with an increase in the mass transfer coefficient with increasing feed flow rate. However, the situation is reversed at very high bulk protein concentrations, with the flux ratios becoming

greater than one at a bulk concentration between 100 and 150 g/L. This corresponds to the point where the exit transmembrane pressure drop at the higher feed flow rate (65 mL/min) approaches a value of zero due to the large feed–side pressure drop through the module (Figure 11). Under these conditions, the filtrate flux is actually greater at the lower feed flow rates, which is completely opposite of what is expected based on the concentration polarization model. These data clearly demonstrate the importance of the feed–side pressure drop in determining the filtrate flux at high protein concentrations, with the large viscosity under these conditions leading to very low flux (or even back–filtration) near the device exit which significantly reduces the length–average flux under these conditions.

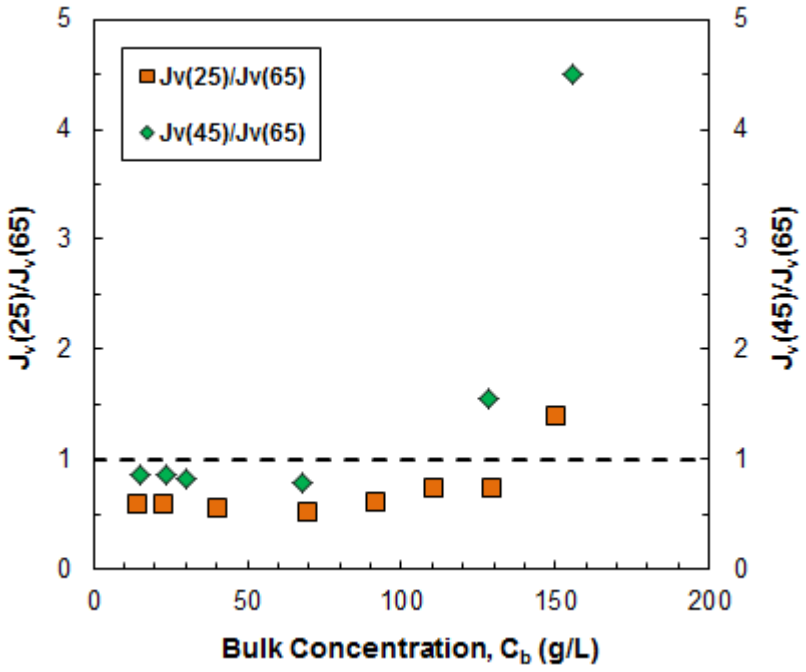

Figure 12: Flux ratios of 25 and 45 mL/min to 65 mL/min vs bulk concentration

4.3 Modified Batch Filtration Experiments

To reduce the number of experiments and conserve valuable protein, the standard batch experiments were modified so that flux data could be obtained at multiple feed flow rates (e.g., 35, 45, and 55 mL/min) as part of a single experimental run. This also eliminates artifacts associated with sample–to–sample variations in the protein feed solution or to small differences in the Pellicon 3 modules. Figure 13 shows results from one of the modified batch filtration experiments (closed symbols). In this case, the experiment began using a feed flow rate of 45 mL/min. Two flux data points were obtained at this value of q, with the feed flow rate then rapidly increased to 55 mL/min. Two flux measurements were taken at this new feed flow rate, at which point q was decreased to 35 mL/min. This procedure was repeated multiple times, with the feed flow rate sequentially changed from 35 to 45 to 55 mL/min and then back to 35 mL/min. The filtrate flux data in this experiment were nearly equivalent to those obtained in the standard batch filtration experiments (open symbols). For example, the flux at a feed flow rate of 45 mL/min in the standard batch filtration was 7.0 μm/s at C_b = 48 g/L, while that in the modified batch experiment was 6.8 μm/s at C_b = 55 g/L.

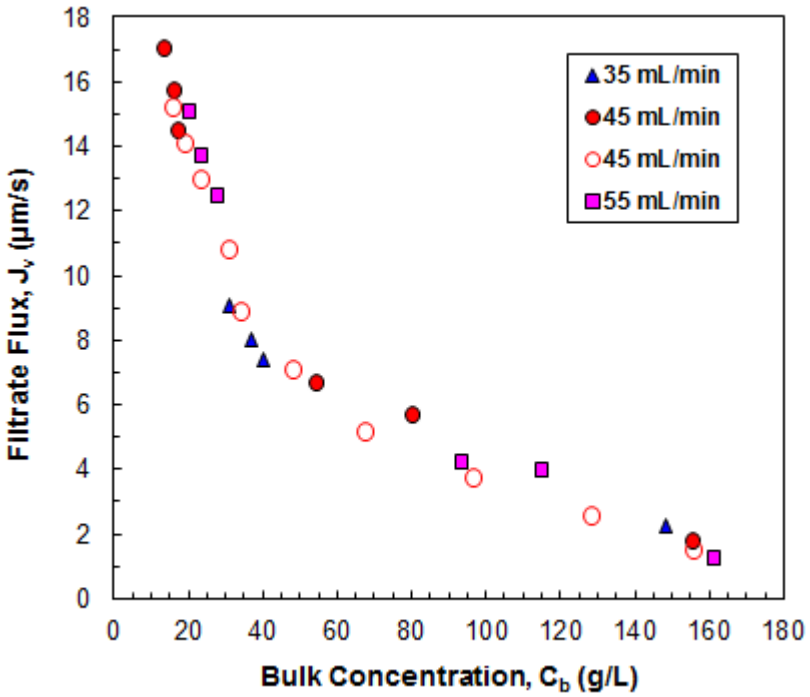

Figure 13: Comparison of standard and modified batch filtration results (5 mM sodium acetate, 20 mM NaCl, pH 5)

The modified back filtration experiments were used to examine the filtrate flux in different buffer conditions. In each case, the stagnant film model (Equation 2) was used to determine the best fit values of the maximum wall concentration and mass transfer coefficient using a simple linear regression on the semi–log plot as shown in Figure 14. The results are summarized in Table 3 along with the values of the second virial coefficient determined by self–interaction chromatography as described in Binabaji et al. [10].

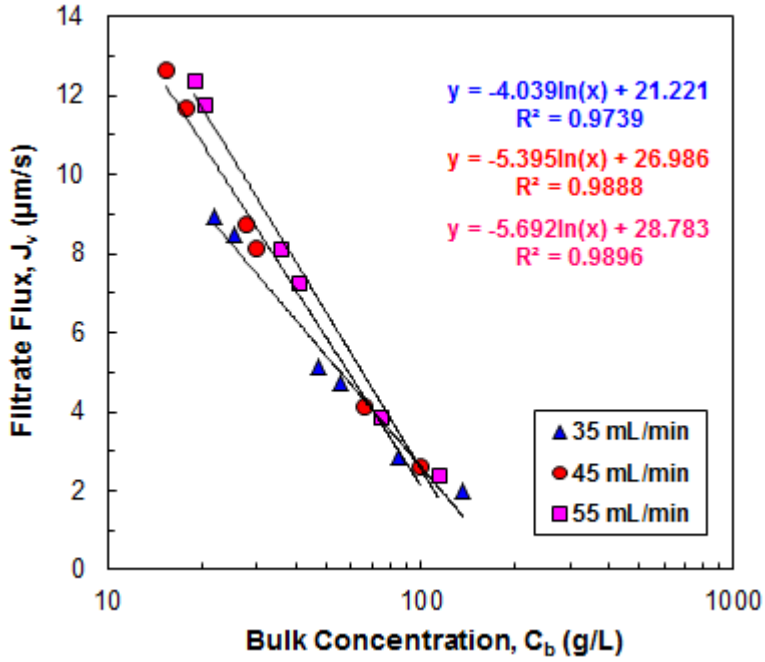

Figure 14: Modified batch filtration results for 3 different feed flow rates (5 mM sodium phosphate, 20 mM NaCl, pH 7)

Table 3: Modified batch filtration results for all buffer conditions.

Buffer Condition	Feed Flow Rate (mL/min)	Max C_w (g/L)	k_m (µm/s)	B_2 ($m^3 \cdot mol/kg^2$) × 10^4
5 mM Sodium Acetate 20 mM NaCl, pH 5 (BC1)	35	250	4.2	3.1 ± 0.3
	45	190	6.2	
	55	200	6.5	
5 mM Sodium Phosphate 20 mM NaCl, pH 7 (BC2)	35	190	4.0	1.9 ± 0.3
	45	140	5.4	
	55	160	5.7	
5 mM Sodium Acetate 20 mM NaCl 5 mM Sucrose, pH 5 (BC3)	35	190	6.1	3.1 ± 0.3
	45	160	9.3	
	55	160	9.6	
5 mM Sodium Acetate 20 mM NaCl 150 mM Proline, pH 5 (BC4)	35	230	3.9	2.8 ± 0.3
	45	210	4.5	
	55	216.9	4.7	

B_2 values reproduced from [10]

As seen in Table 3, the maximum concentration at the membrane surface (C_w) was greatest at a feed flow rate of 35 mL/min, with very similar values at feed flow rates of 45 and 55 mL/min. The mass transfer coefficient (k_m) increased with increasing feed flow rate as expected, although the values at 45 and 55 mL/min were again fairly similar. The best fit values of C_w and k_m in the 5 mM sodium acetate buffer at pH 5 (BC1) were uniformly larger than those in the 5 mM sodium phosphate buffer at pH 7 (BC2). These differences are likely due to the increase in electrostatic repulsion between the positively–charged antibodies at low pH (where the protein charge is greater at pH 5 than at pH 7 since the isoelectric point of the mAb is around pH 8.1). This is also reflected in the much larger value of the second virial coefficient in the pH 5 solution. The addition of 5 mM sucrose (BC3) caused an apparent reduction in C_w but a large increase in k_m, leading to higher values of the filtrate flux at all but the highest bulk concentrations. In contrast, the addition of 150 mM proline (BC4) caused an increase in C_w and a reduction in k_m. The origin of these changes in flux, wall concentration, and mass transfer coefficient in the different buffers is currently under investigation.

One possible source of error in these experiments was a change in the protein solution over time. The protein solution tended to become “cloudy” during the ultrafiltration run leading to significant irreversible fouling and a reduction in the membrane permeability over the course of the filtration. It might be possible to obtain additional insights into this phenomenon by examining the protein solution via size–exclusion chromatography to detect the presence of dimers and higher order oligomers. It might also be useful to probe the secondary structure of the protein before and after each experiment using UV Circular Dichroism.

Chapter 5

Stirred Cell Ultrafiltration Experiments

The filtrate flux behavior in the tangential flow filtration module is complicated by the variation in the transmembrane pressure drop with position along the length of the module. This effect is particularly pronounced at high protein concentrations due to the high viscosity of the antibody solution. For example, the transmembrane pressure drop (P_F–P_R) varied from 30 psi at the device inlet to 0 psi at the retentate exit for experiments with concentrations >100 g/L.

In order to obtain additional insights into the ultrafiltration behavior at high protein concentrations, a series of experiments were performed in a stirred ultrafiltration cell in which the transmembrane pressure drop was essentially uniform over the surface of the membrane. In this case, data were obtained using a standard batch process, i.e., as a function of time as the antibody concentration increases, with experiments performed at different stirring speeds to vary the bulk mass transfer coefficient. All experiments used the baseline buffer condition: 5 mM sodium acetate and 20 mM NaCl at pH 5.

Experimental results at stirring speeds of 300 and 600 rpm at a transmembrane pressure drop of 8.5 psi are shown in Figure 15. The filtrate flux decreases with increasing antibody concentration with an approximately linear dependence on ln(C_b), similar to the behavior seen in Chapter 4. The data at 600 rpm are uniformly larger than those at 300 rpm, consistent with the increase in bulk mass transfer coefficient associated with the greater stirring speed. This effect is most pronounced at high protein concentrations. For example, the filtrate flux at a bulk protein concentration of 190 g/L is 0.74 μm/s at 600 rpm but this drops to only 0.23 μm/s as the stirring speed was reduced to 300 rpm.

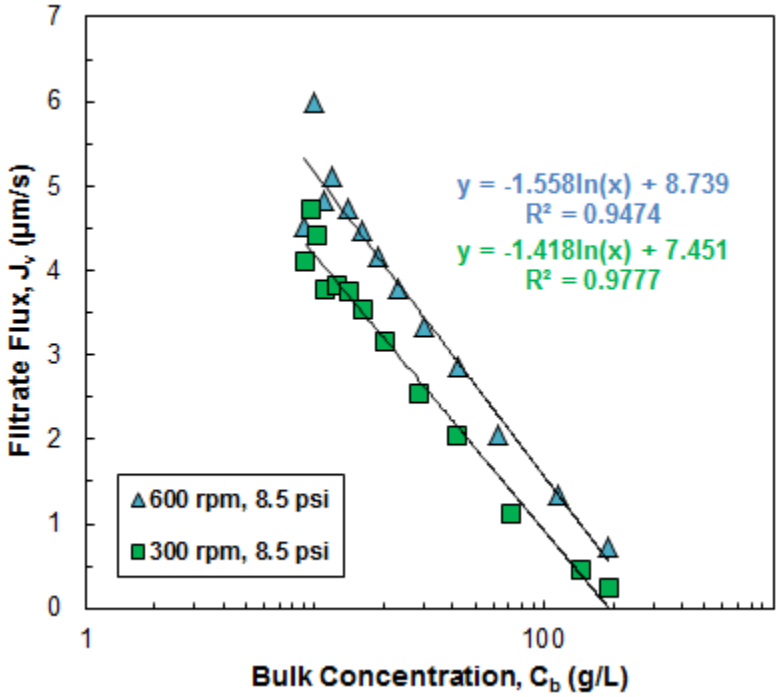

Figure 15: Stirred cell ultrafiltration results for two different stirring speeds

The stagnant film model (Equation 2) was again used to estimate the maximum protein concentration at the surface of the membrane (C_w) and the mass transfer coefficient (k_m), with the best fit values of the model parameters given in Table 4. The mass transfer coefficient increases with increasing stirring speed as expected, although the dependence on stirring speed is considerably less than that predicted using available theoretical models and experimental correlations, which show a dependence of between $\omega^{0.5}$ and $\omega^{0.57}$ [7]. In addition, the calculated value of the wall concentration is considerably larger at the higher stirring speed. This behavior is opposite of that observed in the tangential flow filtration module, where the calculated wall concentration decreased with increasing feed flow rate (i.e., mass transfer coefficient). This difference in behavior is likely due to the large pressure drop along the length of the membrane in the tangential flow filtration device.

Table 4: Best fit values of C_w and k_m in the stirred cell ultrafiltration experiments

Experimental Conditions	Max. C_w (g/L)	k_m (µm/s)
(1) 600 rpm, 8.5 psi	270	1.6
(2) 300 rpm, 8.5 psi	190	1.4

Figure 16 shows the ratio of the filtrate fluxes at the lower stirring speed (300 rpm) to that at the higher stirring speed (600 rpm) as a function of the bulk protein concentration for experiments performed using the same acetate buffer at pH 5. The ratio of fluxes is always below one and decreases nearly linearly with increasing protein concentration. It is important to note that the protein solution used in the experiment at 600 rpm experiment got very foamy at high protein concentrations; this was not observed at 300 rpm. The presence of the foam reduced the effective viscosity of the solution, although it is difficult to know exactly how this might have influenced the filtrate flux.

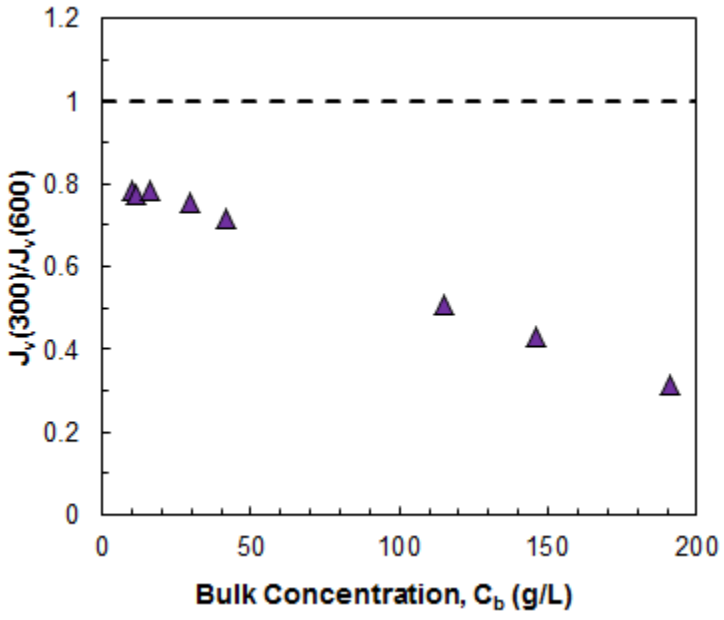

Figure 16: Flux ratio of 300 rpm to 600 rpm vs bulk concentration

Figure 17 shows a comparison of the results in the stirred cell (at 600 rpm) and in the tangential flow filtration system (at feed flow rates of 45 mL/min and 65 mL/min). The transmembrane pressure in the stirred cell was maintained at 8.5 psi while that in the Pellicon 3 TFF module was at 15.5 psi. The filtrate flux in the stirred cell was smaller than that in the TFF module, particularly at low bulk protein concentrations, consistent with the much larger mass transfer coefficient in the tangential flow device [7]. However, the flux ratio clearly increases with increasing concentration, especially for the 65 mL/min TFF experiment where the flux ratio is approximately equal to one at a mAb concentration of 140 g/L. This is due to the reduction in flux in the TFF module associated with the very large transverse pressure drop associated with flow through the tangential flow filtration module, which leads to very small transmembrane pressure drops at the device exit. Under some conditions, this resulted in a negative transmembrane pressure near the retentate exit of the TFF module, which would have generated a negative "back-filtration" in this region of the device.

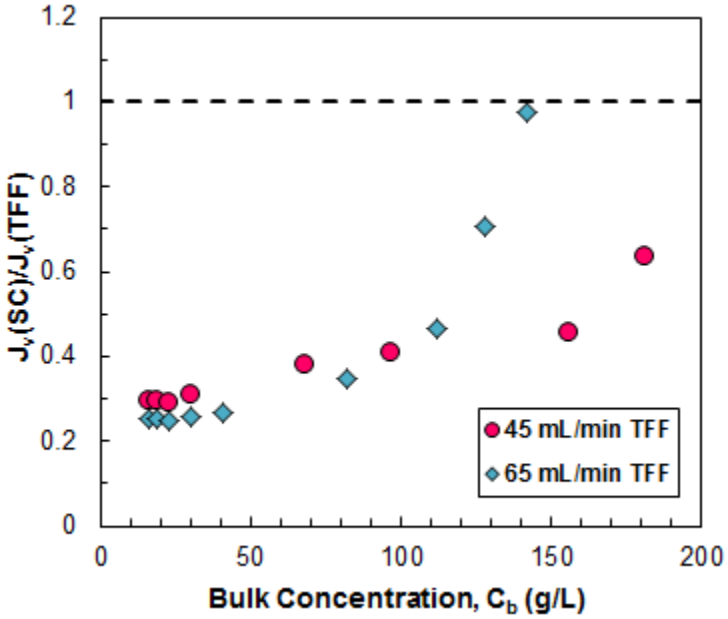

Figure 17: Flux ratio of SC at 600 rpm to TFF at 45 and 65 mL/min vs bulk concentration

Chapter 6

Conclusions

The push for lower production costs, increased development speed, and overall higher productivity in the biotechnology industry has been driving improvements to membrane processes. In addition, there has been a significant trend towards the use of much higher antibody concentrations in final product formulations to achieve the desired therapeutic effect. Therefore, there is a real need to better understand the behavior of membrane processes used for the production of highly concentrated antibody solutions. This thesis presented the most extensive data set currently available on the filtrate flux of highly concentrated monoclonal antibody solutions using a highly purified monoclonal antibody provided by Amgen.

Total recycle experiments were used to illustrate the ultrafiltration behavior at steady state and establish conditions for the pressure–independent regime. Standard batch filtration experiments were conducted over a range of feed flow rates (25 – 65 mL/min). At low protein concentrations, the filtrate flux increased significantly with increasing feed flow rate. However, at higher mAb concentrations (>100 g/L), the effect of feed flow rate on the filtrate flux was much less pronounced. This was likely due to the significant pressure drop for flow through the Pellicon 3 modules; experiments at concentrations above 100 g/L had such a large pressure drop on the feed–side of the module that the exit transmembrane pressure drop was close to zero, leading to a very low or even negative (back–filtration) flux in this region of the module.

Additional data were obtained using a modified batch filtration method, providing results at multiple feed flow rates in a single experiment. Data were analyzed using the classical stagnant film model to evaluate the mass transfer coefficient and the maximum wall

concentration. The mass transfer coefficient (k_m), increased with increasing feed flow rate as expected. Interestingly, the maximum concentration at the membrane surface (C_w) was greatest at the lowest feed flow rate (35 mL/min) under all conditions. This may also be due to the large feed–side pressure drop, which increased with increasing feed flow rate. The C_w and k_m values were also a function of the buffer conditions, with much larger values at pH 5 than at pH 7 due to the strong electrostatic repulsive interactions between the more highly charged antibody molecules at low pH. This was consistent with the much larger value of the second virial coefficient (B_2). The addition of sucrose and proline also had a significant effect on the filtrate flux, mass transfer coefficient, and wall concentration, although more detailed experimental studies will be required to identify the origin of these changes.

The filtrate flux behavior in the tangential flow filtration module is complicated by the variation in the transmembrane pressure drop with position along the length of the module, an effect that is increasingly important for more highly concentrated protein solutions due to the large viscosity. Therefore, a series of ultrafiltration experiments were performed using a stirred cell in which the transmembrane pressure drop was essentially uniform over the surface of the membrane. It was found that the mass transfer coefficient increased with increasing stirring speed as expected, although the dependence on stirring speed was less than that predicted using available theoretical models and experimental correlations. The maximum wall concentration, on the other hand, decreased with decreasing stirring speed, which is exactly the opposite of the behavior seen in the TFF experiments. The ratio of the filtrate fluxes in the stirred cell to that in the TFF module increased with increasing protein concentration, providing additional support for the hypothesis that the large transverse pressure drop in the TFF module has a large effect on the ultrafiltration behavior.

Future studies should be performed to provide more quantitative information on the underlying mechanisms controlling the filtrate flux and the maximum achievable protein concentration in an ultrafiltration process. This would include additional results for the dependence of the maximum wall concentration and the mass transfer coefficient on both the feed flow rate and buffer conditions. In addition, it would be very interesting to obtain data in other TFF devices that have different transverse pressure drops, e.g., devices with different channel dimensions or with different internal spacers in the feed channel. These data would provide additional insights into the effects of the transverse pressure drop on the ultrafiltration behavior at very high protein concentrations, i.e., at very high viscosities.

Chapter 7

Bibliography

1. Zydney, A.L. (2009). Membrane technology for purification of therapeutic proteins. Biotechnol. Bioeng., 103(2): 227–230.

2. Reichert, J.M., Rosensweig, C.J., Faden, L.B., Dewitz, M.C. (2005). Monoclonal antibody successes in the clinic. Nat. Biotechnol., 23(9): 1073–1078.

3. Reichert, J.M. "Therapeutic Monoclonal Antibodies Approved or in Review in the European Union or United States." The Antibody Society. The Antibody Society, 28 Jan. 2014. <http://www.antibodysociety.org/news/approved_mabs.php>.

4. van Reis, R., Zydney, A.L. (2007). Bioprocess membrane technology. J. Membr. Sci., 297: 16–50.

5. Kurnik, R. T., Yu, A.W., Blank, G.S., Burton, A.R., Smith, D., Athalye, A. M., van Reis, R. (1995). Buffer exchange using size exclusion chromatography, countercurrent dialysis, and tangential flow filtration: Models, development, and industrial application. Biotechnol. Bioeng., 45(2): 149–157.

6. Mehta, A., Zydney, A.L. (2005). Permeability and selectivity analysis for ultrafiltration membranes. J. Membr. Sci., 249: 245–249.

7. Zeman L.J., Zydney A.L. (1996). Microfiltration and Ultrafiltration: Principles and Applications. New York: Marcel Dekker, Inc.

8. Perkins T.W., Saksena S., van Reis R. (1999). A Dynamic film model for ultrafiltration. J. Membr. Sci., 158(1-2): 243–256.

9. Vilker, V.L., Colton, C.K., Smith, K.A., Green, D.L. (1984). The osmotic pressure of concentrated protein and lipoprotein solutions and its significance to ultrafiltration. J. Membr. Sci., 20(1): 63–77.

10. Binabaji, E., Rao, S., Zydney, A.L. (2014). The osmotic pressure of highly concentrated monoclonal antibody solutions: effect of solution conditions. Biotechnol. Bioeng., 111: 529–536.

11. Wu, J., Prausnitz, J.M. (1999). Osmotic pressures of aqueous bovine serum albumin solutions at high ionic strength. Fluid Phase Eq., 155(1): 139–154.

ACADEMIC VITA

Stephanie Nitopi
254 Terrace Ave
Hasbrouck Heights, NJ 07604
201-446-5511
stenit11@gmail.com, snitopi@stanford.edu

Education

The Pennsylvania State University, University Park, PA — *Aug 2009–May 2014*
B.S. in Chemical Engineering
Schreyer Honors College

Honors and Awards

Stanford Graduate Fellowship	*2014–2017*
Merck Engineering & Technology Fellowship Award	*2013–2014*
The Evan Pugh Scholar Award – Senior Award	*Spring 2013*
Undergraduate Research Fellowship in Biomolecular Engineering	*Summer 2012*
The Evan Pugh Scholar Award – Junior Award	*Spring 2012*
The President Sparks Award	*Spring 2011*
The President's Freshman Award	*Spring 2010*
Schreyer Honors College Academic Excellence Scholarship	*2009–2013*

Research Experience

Associate Specialist, Engineering Intern–Merck — *June 2013–Aug 2013*
Chemical Process Development & Commercialization Department

The Department of Chemical Engineering at Penn State — *Jan 2012–May 2014*
Membrane Processes Research under Dr. Andrew Zydney

The Applied Research Lab at Penn State — *Jan 2011–May 2011*
Bioacoustics research under Dr. Susan Parks

Work Experience

Teaching Intern–CH E 210: Introduction to Material Balances — *Aug 2013–Dec 2013*
Faculty Supervisor: Dr. Janna Maranas, Associate Professor of Chemical Eng.

Global Procurement Co-op–Bristol-Myers Squibb — *Jan 2013–June 2013*

Resident Assistant–The Pennsylvania State University — *Jan 2012–Dec 2012*

Teaching Aid–MATH 251: Ordinary and Partial Diff. Eqns. — *Aug 2011–Dec 2011*
Faculty Supervisor: Zachary Tseng, Instructor, MATH 251 Course Coordinator